ELSEVIER

Journal of Food Engineering **37** (1998) 111–125
© 1998 Elsevier Science Limited. All rights reserved
Printed in Great Britain
0260-8774/98/$19.00+0.00

PII: S0260-8774(98)00087-9

Prediction of Chilling Times of Foods in Situations Where Evaporative Cooling is Significant—Part 1. Method Development

Sawitri Chuntranuluck,[a] C. M. Wells[b] & A. C. Cleland[c]*

[a]Biotechnology Department, Kasetsart University, Bangkok, 10900, Thailand
[b]Agriculture New Zealand Ltd, PO Box 8640, Christchurch, New Zealand
[c]College of Sciences, Massey University, Private Bag 11-222, Palmerston North, New Zealand

(Received 22 September 1997; accepted 26 May 1998)

ABSTRACT

The finite difference method was used to simulate the unsteady state cooling of spheres, infinite slabs and infinite cylinders of food materials subject to both convection and evaporation at the product surface. Simulations were conducted across wide ranges of air temperature, surface heat transfer coefficient, product initial temperature, surface water activity and air relative humidity. Algebraic equations are proposed for finding three parameters—the product equilibrium temperature as time $\rightarrow \infty$*, a slope parameter of semi-log plots relating unaccomplished temperature change to time and an intercept parameter of the same plots. The first of these equations is based on psychrometric theory and the other two were derived by using non-linear regression to curve-fit the numerically simulated cooling rates. These equations allow the numerically simulated cooling times to be predicted within about* $\pm 5\%$*. In Part 2 the accuracy of these equations as a simple chilling time prediction method is tested experimentally for model food systems. In Part 3 their application to real foods is considered.* © *1998 Elsevier Science Limited. All rights reserved*

NOMENCLATURE

a_w Water activity at product surface

*Author to whom correspondence should be addressed.

Bi	Biot number ($h\,R\,k^{-1}$)
c	Specific heat capacity (J kg^{-1} K^{-1})
f	Slope of a plot of ln Y vs Fo
E	Shape parameter; = 0·75 (infinite slab); = 1·76 (infinite cylinder); = 3 (sphere)
Fo	Fourier number ($k\,t\,\rho^{-1}\,c_p^{-1}\,R^{-2}$)
h	Surface heat transfer coefficient (W m^{-2} K^{-1})
H	Humidity ratio
j	Lag factor or intercept of a plot of ln Y vs Fo
k	Thermal conductivity (W m^{-1} K^{-1})
K	Mass transfer coefficient (kg s^{-1} m^{-2} Pa^{-1})
n	Shape parameter; = 1 (infinite slab); = 2 (infinite cylinder); = 3 (sphere)
p	Partial pressure of water vapour in air (Pa)
P	Total air pressure (Pa)
r	Space position within product (m)
R	Characteristic length (radius) of product (m)
t	Time (s)
T	Temperature (°C)
Y	Dimensionless temperature
β	First root of a transcendental equation
ε	Latent heat of vaporisation of water (J kg^{-1})
ρ	Density of product (kg m^{-3})

Subscripts

a	Air
av	Mass-average
c	Centre
Conv	Convection only
eq	Equilibrium
Evap	Evaporation and convection
in	Initial
m	Space position in r direction in numerical calculations
M	Space position at outer edge of product
p	Product
r	Relative (humidity)
w	Saturation

Superscript

i	Number of time step or time level in numerical calculations

INTRODUCTION

There are many situations in which the chilling rate of foods cooled in an air stream is accelerated by the loss of moisture from the product surface and the associated removal of the latent heat of evaporation. In a typical chilling process for meat, fish, vegetables or fruit the product might cool by about 30°C and the energy loss is of

the order of 100 kJ kg^{-1}. If a 1% weight loss occurs the evaporative contribution would be about 25%. Weight losses higher than 1% occur in some commercial food chilling processes. Therefore, if accurate predictions of chilling time are to be made in such circumstances the evaporation must be directly considered in the prediction methodology.

The relatively low thermal conductivity and considerable thickness of some food products means that conduction from the innermost tissues to the surface must be considered as well as the surface heat transfer. The basic law of heat transfer by conduction is Fourier's law. For the three simplest shapes (the infinite slab $-R \leq r \leq R$, the infinite cylinder $0 \leq r \leq R$, and sphere $0 \leq r \leq R$), with constant product thermophysical properties:

$$\rho c_p \frac{\partial T}{\partial t} = k \frac{\partial^2 T}{\partial r^2} + (n-1) \frac{k}{r} \frac{\partial T}{\partial r} \tag{1}$$

For a uniform initial product temperature:

$$T = T_{in} \quad \text{for} \quad 0 \leq r \leq R \text{ at } t = 0 \tag{2}$$

For all three shapes the boundary condition at position $r = 0$ can be stated as:

$$\frac{\partial T}{\partial r} = 0 \quad \text{at } r = 0 \text{ for } t \geq 0 \tag{3}$$

At the boundary $r = R$, for $t > 0$ energy transfer takes place due to the combined effect of heat and mass transfer. The boundary condition can be stated as (Gaffney *et al.*, 1985):

$$\left(k \frac{\partial T}{\partial r}\right)_{r=R} = h(T_M - T_a) + K_a(p_M - p_a)\varepsilon \quad \text{at } r = R \text{ for } t \geq 0 \tag{4}$$

The partial pressure of water vapour in the boundary layer over the product surface is defined by:

$$p_M = a_w p_{wM} \tag{5}$$

The partial pressure of water vapour in the bulk air is given by:

$$p_a = H_r p_{wa} \tag{6}$$

Therefore eqn (5) can be rewritten as:

$$\left(k \frac{\partial T}{\partial r}\right)_{r=R} = h(T_M - T_a) + K_a(a_w p_{wM} - H_r p_{wa})\varepsilon \tag{7}$$

In order to solve eqn (7) it is common practice to use the well-known Lewis relationship to inter-relate K_a and h. The Lewis relationship states that for fully developed turbulent flow the heat and mass transfer coefficients are in direct proportion to each other, and for air the Lewis number itself is close to unity. Daudin and Swain (1990) showed that for air velocities above about 0·6 m s^{-1} the Lewis relationship held, and departure from it at lower velocities was due to radiation influences when the surrounding structures were at the ambient air temperature. Such radiation influences are less likely to be significant in industrial chillers holding many items at the same temperature than in a pilot plant chiller holding an indivi-

dual item. Hence the error in neglecting radiation is often less than Daudin and Swain found. An interpretation (Chuntranuluck, 1995) of the Lewis relationship for the above nomenclature is:

$$\frac{h}{K_a} \approx \frac{29c_aP}{18} \tag{8}$$

This interpretation assumes that the partial pressure of water vapour in the air stream is small in comparison to the total air pressure; a reasonable assumption for most chilling problems as the vapour pressure of water at 20°C, a maximum likely air temperature in chilling, is only about 2% of atmospheric pressure.

In attempting to solve this set of equations, or the more complex equivalents that apply for other shapes, a major difficulty lies in the form of eqn (7). The vapour pressure of water at the product surface temperature varies nonlinearly with the temperature of the surface. Further, and more importantly, a_w depends on the surface water concentration, which itself depends on the rate of water movement to the product surface (by diffusion or capillary action), the presence or otherwise of a 'skin' layer and the rate of evaporation.

Numerical methods allow the solution of eqns (1)–(8) without the introduction of significant errors in the solution method. Such solutions attempt to model the real change of a_w with time. However, as has been found by Radford *et al.* (1976), James *et al.* (1988) and Campanone *et al.* (1995) amongst others, major effort is required to model the moisture movement within the product, particularly in obtaining data which are often product-specific. Hence, the apparent benefits of attempting to model the heat and mass transfer processes in a physically accurate manner are difficult to realise in practice. This suggests that approximate solutions to eqns (1)–(8) may be adequate provided that the error introduced by the method of solution is not large.

A recent review by Kuitche *et al.* (1996a,b) summarises the various approaches taken. Those deriving simple, approximate prediction methods have made assumptions about the value of a_w during the process. A common assumption has been that $a_w = 1{\cdot}0$ (Srinivasa Murthy *et al.*, 1976; Abdul Majeed *et al.*, 1980). The assumption that $a_w = 1$ is appropriate for some types of product, particularly those whose surfaces would not be exposed to air in nature and hence which do not have natural water loss protection. Thus, for chilling of animal carcasses with skin removed or cut meat surfaces, this model is expected to perform well. Recent examples of its application include the work of Daudin and Kuitche (1995) and Kuitche and Daudin (1995) for pork and rabbit carcasses, respectively. For products of lower moisture content, or with natural protection, it is not appropriate to make this assumption. For example, Campanone *et al.* (1995) found that unwetted apples cooled about 20% slower than apples with wetted surfaces (for which $a_w = 1$ is a reasonable assumption).

Once the assumption of a fully wetted surface is made, it has been common to lump the evaporative component of eqn (7) in with the convective component by inflating the numerical value of h by an appropriate amount. Daudin and Kuitche (1995) suggest that an appropriate multiplier is about 4 at the onset of a process in which the product starts at 40°C but as low as 2 towards the end of the same process. The controlling processes are thus modelled entirely as heat transfer. Following this approach, Kuitche *et al.* (1996a,b) developed a generalised step-wise

methodology for cases with $a_w = 1$. This method re-estimates an 'effective' *Bi* value at each step. The effective *Bi* includes the evaporative effect. The final equilibrium temperature of the product was assumed to be the wet bulb temperature. The method was tested against data for a wet plaster model system. The method is not suitable for hand computation as it requires a number of time steps to be calculated. If the assumption that $a_w = 1$ is not valid then it is implied that a different *Bi* determination would be required, but this was not quantified.

For products with skins another possibility is to model the mass transfer resistance of the skin (by including it in K_a) but to ignore the water storage within the skin (Chau *et al.*, 1985). If this approach is taken it is often assumed that the a_w of the underlying tissue is constant and high (approaching 1·0).

There would be practical benefits to those working in the industrial community from the development of a methodology which had low data requirements, was simple to use (e.g. avoiding computer programming) and widely applicable. The method should be heat transfer-based and thus not require the user to have detailed knowledge of mass transfer processes within the product. It should cover a_w values well below 1·0, thus differentiating it from many previous studies including that of Kuitche *et al.* (1996a,b). Because others have found the approach successful for $a_w = 1$, the starting point for developing the new prediction method was chosen as the analytical solutions to eqns (1)–(8) for situations in which evaporation was absent. The specific objective was then to develop means for scaling results from these solutions in a manner which enabled the effect of evaporation to be included, but also allowed the assumption of $a_w = 1{\cdot}0$ to be relaxed. If possible, the means of scaling would require no more than algebraic equations and avoid computer programming in its implementation.

In Part 1, the theoretical development of the methodology is described. In Part 2, experimental testing for a food analogue material with constant surface water activity is reported. Part 3 considers application to real foods. This work considers only the three basic shapes and situations in which surface water activity could be modelled as a constant (but not necessarily equal to unity). It considers a wide range of product initial temperature, ambient temperature and relative humidity conditions. Such circumstances are still somewhat restrictive, but if a simple and accurate methodology could not be developed for such circumstances there appeared to be no advantage in seeking a method for less restrictive conditions.

DEVELOPMENT AND USE OF A NUMERICAL MODEL

Whilst the aim of the present work is to develop an algebraic means of scaling chilling time predictions to take account of evaporation at the product surface, this did not preclude the use of numerical methods to help in the analysis. It was anticipated that accurate experimental data collection would be difficult. Therefore, it was decided to use numerical methods to predict likely behaviour and then base simple model development on fit to the numerically predicted results. The experimental data could then be used solely for model testing and not for model development.

For simplicity, an explicit finite difference method was selected to solve eqns (1)–(8). The first node, $m = 0$, was placed at the centre of the solid and the highest numbered node, M, at the solid surface. The node in each volume element is at the

midpoint between the two surfaces of the element, except for the outermost and innermost elements which have thicknesses of $\Delta r/2$ and in which the node is at one edge of the element. Evaporative and convective heat transfer occur from the outer surface of the Mth element. Heat balances for the various regions were used to derive appropriate formulae. For a generalised region $1 \leq m \leq M-1$, $t > 0$:

$$\frac{T_m^{i+1} - T_m^i}{\Delta t} = \frac{k}{\rho c_p} \frac{\left[1 + \left(\frac{n-1}{2m}\right)\right] T_{m+1}^i - 2T_m^i + \left[1 - \left(\frac{n-1}{2m}\right)\right] T_{m-1}^i}{\Delta r^2} \tag{9}$$

The boundary condition at $r = R$ ($m = M$) for $t > 0$ is given by:

$$\frac{\rho c_p}{n}\left(\frac{T_M^{i+1} - T_M^i}{\Delta t}\right) = \frac{1}{\left[M^n - \left(M - \frac{1}{2}\right)^n\right]\Delta r}\left[\left(M - \frac{1}{2}\right)^{n-1} \frac{k}{\Delta r}(T_{M-1}^i - T_M^i) - M^{n-1}h(T_M^i - T_a) - M^{n-1}K_a\varepsilon(p_M^i - p_a)\right] \tag{10}$$

For the boundary at $r = 0$ ($m = 0$) and for $t > 0$, symmetry considerations suggest:

$$\frac{\rho c_p}{2n}\left(\frac{T_0^{i+1} - T_0^i}{\Delta t}\right) = \frac{k}{\Delta r^2}(T_1^i - T_0^i) \tag{11}$$

The uniform initial condition at $t = 0$ is:

$$T_m = T_{in} \quad \text{at} \quad t = 0 \quad \text{for} \quad 0 \leq m \leq M \tag{12}$$

The mass-average temperature is found by weighting nodal temperatures according to their associated masses (volumes) of material:

$$T_{av} = \frac{\sum_{m=0}^{M} [(\text{volume of element around node } m)\ (\text{temperature at node } m)]}{\sum_{m=0}^{M} (\text{volume of element around node } m)} \tag{13}$$

$$T_{av} = \frac{\left[M^n - \left(M - \frac{1}{2}\right)^n\right] T_M + \frac{T_0}{2^n} + \sum_{m=1}^{M-1}\left[\left(m + \frac{1}{2}\right)^n - \left(m - \frac{1}{2}\right)^n\right] T_m}{M^n} \tag{14}$$

The saturation vapour pressure of water p_{wM} and p_{wa} can be satisfactorily approximated from T_M and T_a, respectively using an Antoine equation:

$$p_w \approx \exp\left(23{\cdot}4795 - \frac{3990{\cdot}56}{T + 233{\cdot}833}\right) \tag{15}$$

The latent heat of vaporisation was approximated by:

$$\varepsilon \approx 2{\cdot}5 \times 10^6 - 2{\cdot}5 \times 10^3 T_M \tag{16}$$

Equations (9)–(16) were programmed in the PASCAL programing language. To confirm programming accuracy, predictions made using the computer program were compared to predictions made using the analytical solutions to eqns (1)–(7) for the case where there was no evaporation. Time and space steps were set sufficiently small to make numerical errors small—10 space steps in the radius, and a time step of about half the maximum possible for numerical stability (Cleland, 1990). A variety of situations with evaporation occurring were then simulated. The range of conditions covered were:

T_a (°C)	0, 5, 10, 15
T_{in} (°C)	20, 30, 40, 50
Bi	0.1, 0·316, 1·0, 3·16, 10
a_w	0.6, 0·8, 1·0
H_r	0.5, 0·75, 1·0
Shape	infinite slab, infinite cylinder, sphere

For each combination, the simulation was repeated with convection only and with cooling by both evaporation and convection.

SIMPLE MODEL DEVELOPMENT

For the three simplest shapes (infinite slab, infinite cylinder and sphere), when cooling occurs by convection only, there are well-known analytical solutions that express the variation of product temperature (T) with time (t) and other thermophysical parameters provided the initial product temperature is uniform; ambient conditions and thermal properties are constant; and internal heat transfer is totally by conduction. The form of these analytical solutions is an infinite series in which, except at short times, only one term is significant. Most practical chilling processes meet this criterion and the so-called one term approximation is used:

$$Y = \frac{(T - T_a)}{(T_{in} - T_a)} \approx j_{Conv} \exp[-\beta^2 kt/(\rho c_p R^2)] \approx j_{Conv} \exp(-f_{Conv} Fo) \qquad (17)$$

When ln Y is plotted against Fo, a straight line of slope $-f_{Conv}$ is obtained, with T approaching T_a, the equilibrium temperature, as $t \to \infty$ exponentially. However, when evaporation is introduced linear plots are no longer obtained (Fig. 1). The extent of curvature of the plot depends on the true equilibrium temperature reached as $t \to \infty$ (which is no longer T_a and which depends on both a_w and H_r as Fig. 2 shows). When *Bi* was held constant, the rate of cooling at $H_r = a_w$ was faster than the rate for convection-only cooling. However, the magnitude of the change in rate depended on other conditions, for example, the higher a_w was, the faster the cooling rate (because there was more water available at the product surface, resulting in a stronger evaporative cooling effect).

In trying to linearise the semi-log plots, previous workers have attempted to use wet bulb temperature as the equilibrium temperature because it combines the effects of dry bulb temperature and relative humidity into a single parameter (Earle & Fleming, 1967; Abdul Majeed *et al.*, 1980; Daudin & Kuitche, 1995; Kuitche *et al.*, 1996a,b). Unfortunately, this selection of equilibrium temperature implies that

$a_w = 1$, an assumption rejected in the present work. Hence, the equilibrium temperature was defined by solving eqn (7) at steady state:

$$K_a(a_w p_{wM} - H_r p_{wa})\varepsilon = h(T_a - T_{eq}) \tag{18}$$

which by use of eqn (8) implies that:

$$T_{eq} \approx T_a - \frac{18\varepsilon}{29c_a}\left(\frac{p_M - p_a}{P}\right) \approx T_a - \frac{18\varepsilon}{29c_a}\left(\frac{a_w p_{wM} - H_r p_{wa}}{P}\right) \tag{19}$$

At equilibrium, the surface of the product is at T_{eq}, so ε can be evaluated by substituting T_{eq} in eqn (16). Similarly, p_{wM} can be evaluated by substituting T_{eq} for T in eqn (15). Using eqn (19) and the equations stated earlier for the physical properties of water it follows that:

$$T_{eq} \approx T_a - \frac{18(2{\cdot}5 \times 10^6 - 2{\cdot}5 \times 10^3 T_{eq})}{29c_a P}$$
$$\times \{a_w \exp[23{\cdot}4759 - (3990{\cdot}56/T_{eq} + 233{\cdot}833)]$$
$$- H_r \exp[23{\cdot}4759 - (3990{\cdot}56/T_a + 233{\cdot}833)]\} \tag{20}$$

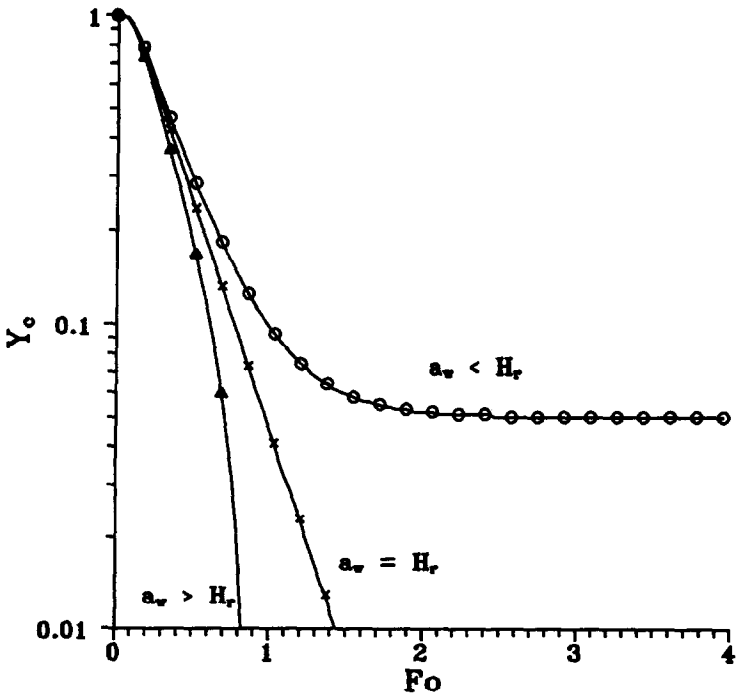

Fig. 1. Example plot of ln Y_c vs Fo for situations in which cooling is by both evaporation and convection, and eqn (17) is used to define Y_c.

T_{eq} is the only unknown and so eqn (20) can be solved iteratively. Using T_{eq} thus defined, the definition of Y was changed to:

$$Y = \frac{(T - T_{eq})}{(T_{in} - T_{eq})} \approx j_{Evap} e^{-f_{Evap} Fo} \tag{21}$$

Equation (20) is consistent with the observed behaviour in Fig. 2. Where $a_w = H_r$ no evaporation occurs at steady state and the equilibrium temperature is the ambient air temperature. In contrast, where $a_w > H_r$ evaporation still occurs at steady state and the equilibrium temperature is less than the ambient air temperature because heat removal by evaporation is being balanced by heat gain by convection. Conversely, where $a_w < H_r$ condensation on the product surface occurs at steady state so the equilibrium temperature is higher than the ambient air temperature.

Using T_{eq} from eqn (20), plots of the form of Fig. 1 became sufficiently linearised for the assumption of linearity to be made without introducing significant error (Figs 3 and 4). (This finding was at variance with the work of Kuitche *et al.* (1996a,b) who changed *Bi* and, by inference, the slope of the semi-log plot continuously during their time-stepping procedure). It was then possible to determine, from semi-log plots of the numerical data, values of the slope with evaporation ($-f_{Evap}$), and the

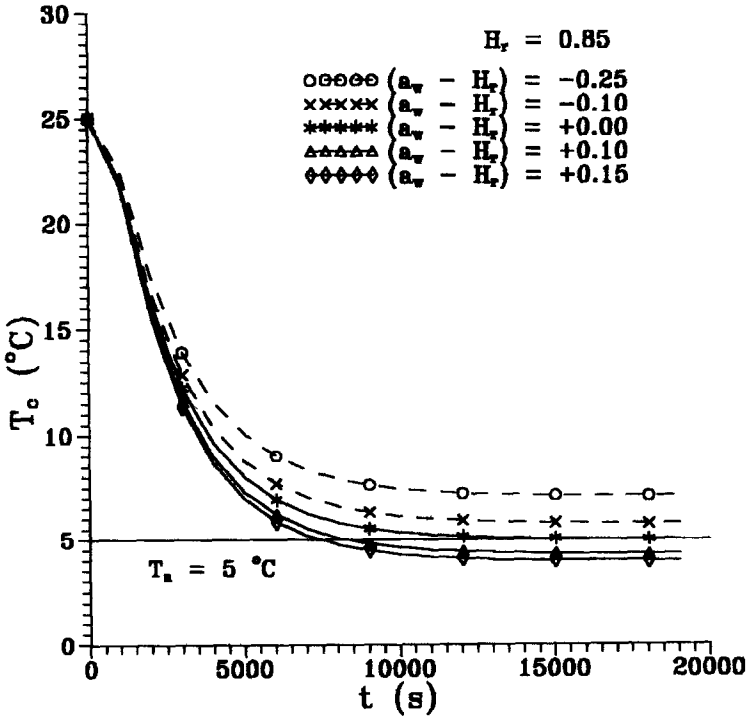

Fig. 2. Example plot of object centre temperature vs time for cooling of cylinders subject to both convection and evaporation/condensation at the product surface.

intercept with evaporation (j_{Evap}) for both the thermal centre and mass average positions. Ratios of these f and j values to those with convection only, under otherwise the same conditions, were then calculated. This led to data sets relating the ratio of f and j values to environmental conditions.

The magnitude of the evaporative cooling effects depends on the environmental conditions (Bi, T_a, and H_r) and product properties (T_{in} and a_w). Across the ranges tested, the slope of the semi-log plot with evaporative cooling ($-f_{Evap}$) was between 1·1 and 2·9 times that of the convection-only cooling ($-f_{Conv}$) for both centre and mass-average temperatures. The values of the intercepts, j_{cEvap} and j_{avEvap}, were 0·7–1 times the j values for convective-only cooling.

The next stage was to relate the variations of the ratios of f and j values to the environmental and product conditions. It was considered unlikely that a mechanistic basis for best-fitting algebraic equations could be found so non-linear regression was employed to develop curve-fit equations. In selecting terms to introduce into the regression equation, trend graphs and analysis of variance were employed, but finally a trial and error process, to arrive at a relatively simple equation, proved to be necessary. Chuntranuluck (1995) presents details of the analysis employed. The f values for the centre and mass-average temperatures were sufficiently similar that it was necessary to have only one equation for f. The final equations, which include the use of a product shape factor developed by Lin *et al.* (1993), are:

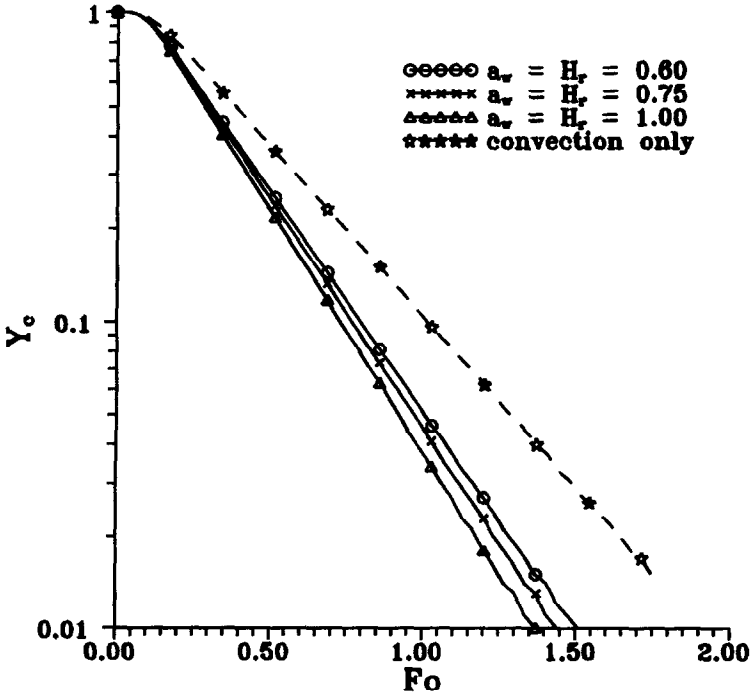

Fig. 3. Example plot of ln Y_c vs Fo for situations in which cooling is by both evaporation and convection, eqn (21) is used to define Y_c, and $a_w = H_r$.

$$\frac{f_{\text{Evap}}}{f_{\text{Conv}}} = 1 + \frac{Bi}{15(Bi^{1.5}+1.5)} + \frac{T_a(H_r+0.34)+(5H_r+0.12T_{in}+9.87)a_w^{0.8}}{19(Bi^{1.2}+1.2)} \quad (22)$$

$$\frac{j_{\text{cEvap}}}{j_{\text{cConv}}} = 1 - \frac{0.0153a_w^{2.4}}{Bi^{0.4}} + 0.0335\left(\frac{Bi^{4/3}+1.85}{\frac{Bi^{4/3}}{E}+\frac{1.85}{n}}\right)e^{-(Bi-2.5)^2} + 0.0725H_r e^{-(Bi-0.7)^2}$$
$$+ T_a(0.00338H_r + 0.00413e^{-(Bi-0.9)^2}) - T_{in}(0.00447e^{-1.33Bi} + 0.000599) \quad (23)$$

$$\frac{j_{\text{avEvap}}}{j_{\text{avConv}}} = 1 + \frac{(0.0345H_r + 0.00207(T_a - T_{in}) - 0.0228a_w^4)}{Bi^{0.333}} - 0.0321H_r e^{-(Bi-2.5)^2}$$
$$- \left[0.00169T_a + 0.0166\left(\frac{Bi^{4/3}+1.85}{\frac{Bi^{4/3}}{E}+\frac{1.85}{n}}\right)\right]e-(0.1Bi)^2 \quad (24)$$

In making predictions, as well as the data that would normally be required for a convection only chilling process, two new data are required—a_w and H_r. The first step is to find the appropriate slope and intercept parameters for convection only cooling

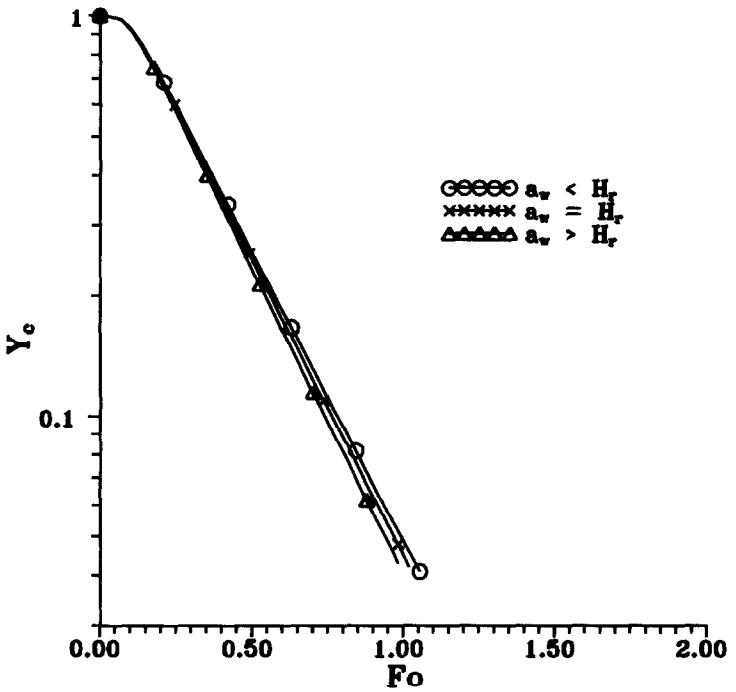

Fig. 4. Example plot of ln Y_c vs Fo for situations in which cooling is by both evaporation and convection, eqn (21) is used to define Y_c, and $a_w \neq H_r$.

(f_{Conv}, j_{avConv} and j_{cConv}). These are found from the analytical solutions of eqns (1)–(7), which are conveniently listed by Cleland (1990). Next, the equilibrium temperature T_{eq} is calculated using eqn (20). Equations (22)–(24) are then used to determine the slope and intercept parameters for cooling with evaporation and convection (f_{Evap}, j_{avEvap}, and j_{cEvap}).

The time to cool to a particular unaccomplished temperature ratio Y is:

$$t = \left(\frac{\ln Y - \ln j_{Evap}}{f_{Evap}}\right)\frac{\rho c_p R^2}{k} \tag{25}$$

whereas the temperature at any time (as represented by *Fo*), is:

$$T = (T_{in} - T_{eq})e^{(-f_{Evap}Fo + \ln j_{Evap})} + T_{eq} \tag{26}$$

Equations (25) and (26) are accurate provided that one-term approximation discussed earlier is valid.

The goal of method implementation without significant computer programming by the user was achieved.

RESULTS AND DISCUSSION

The simple models were tested for the full range of conditions for which numerical solutions were obtained (stated earlier). The percentage differences between the results calculated by the curve-fit algebraic equation and the numerical model were determined:

$$\% \text{ difference} = \frac{(\text{finite difference} - \text{simple model})}{(\text{simple model})} \times 100 \tag{27}$$

The percentage differences in the j_c value, f_c value and time to reach $Y_c = 0{\cdot}1$, 0·35, 0·7 are shown in Table 1. Table 2 shows the equivalent information for the mass-average temperature. One trend in both Tables 1 and 2 is poorer prediction at $Y_c = 0{\cdot}7$ and $Y_{av} = 0{\cdot}55$ than at lower Y values. These observations are explained by consideration of the errors associated with the one term assumption of eqns (17) and (21). As the evaporative effect becomes stronger, it was observed that j_{cEvap} and j_{avEvap} become close to 0·7 and 0·55, respectively. Lower values of Y can occur before the semi-log plot has linearised, thus leading to the poorer fit indicated in Tables 1 and 2. In contrast, with convection-only cooling, j_{cConv} and j_{avConv} depend only on *Bi* and irrespective of *Bi*, $j_{cConv} \geq 1$ and $j_{avConv} \geq 0{\cdot}61$. Therefore, at $Y_c = 0{\cdot}7$ and $Y_{av} = 0{\cdot}55$ the graph has linearised more satisfactorily in even the most extreme conditions.

Without moving to a more complex model than the one term approximation to the series analytical solution for convection cooling, there is no easy way to make the methodology more accurate at higher Y values. $Y_c = 0{\cdot}7$ and $Y_{av} = 0{\cdot}55$ represent practical upper limits. However, at the end of chilling target Y values are usually 0·1–0·3. Thus, the final chilling time will be accurately predicted, generally within 5%. It is postulated that these empirical equations can be used (with high accuracy) for quick estimation of the chilling rate of simple shapes undergoing evaporative

TABLE 1
Percentage Differences Between Results Calculated by the Proposed Curve-fit Algebraic Equations and Results Calculated by Finite Differences for the Centre Temperature of all Three Shapes

Shape		*% difference in* f_{cEvap}/f_{cConv}	*% difference in* j_{cEvap}/j_{cConv}	*% difference in time to* Y_c =		
				0·10	*0·35*	*0·70*
Infinite cylinder	Mean	+0·3	+0·0	−0·2	−0·2	−0·1
	SD	1·5	1·0	1·4	1·6	2·6
	95% conf. interval	−2·7 to +3·2	−1·8 to +1·9	−3·1 to +2·7	−3·3 to +2·9	−5·2 to +5·0
Sphere	Mean	+1·7	+0·5	−1·4	−1·3	−0·8
	SD	2·1	1·9	1·8	1·8	2·9
	95% conf. interval	−2·4 to +5·8	−3·3 to 4·3	−4·9 to +2·1	−4·9 to +2·3	−6·6 to +5·0
Infinite slab	Mean	−1·6	−0·8	+1·3	+0·9	−0·1
	SD	1·7	1·7	1·5	1·6	3·7
	95% conf. interval	−5·0 to +1·8	−4·2 to +2·6	−1·7 to +4·2	−2·1 to +3·9	−7·4 to +7·4

and convective cooling with constant surface water activity over a wide range of practical conditions. This hypothesis is tested in Part 2 (Chuntranuluck *et al.*, 1998a). In Part 3 (Chuntranuluck *et al.*, 1998b) heuristics for extending the method to real food materials are considered.

TABLE 2
Percentage Differences Between Results Calculated by the Proposed Curve-fit Algebraic Equations and Results Calculated by Finite Differences for the Mass-average Temperature of all Three Shapes

Shape		*% difference in* f_{avEvap}/f_{avConv}	*% difference in* j_{avEvap}/j_{avConv}	*% difference in time to* Y_{av} =		
				0·10	*0·35*	*0·55*
Infinite cylinder	Mean	+0·8	+0·1	−0·7	−0·7	−0·5
	SD	1·5	1·1	1·6	2·0	3·1
	95% conf. interval	−2·1 to +3·7	−2·1 to +2·3	−3·8 to 2·4	−4·6 to +3·2	−6·6 to +5·6
Sphere	Mean	+2·7	+0·6	−2·3	−1·9	−1·2
	SD	2·0	1·8	2·3	3·1	5·2
	95% conf. interval	−1·2 to +6·6	−2·9 to +4·1	−6·8 to +2·2	−8·0 to +4·2	−11·4 to +9·0
Infinite slab	Mean	−1·6	0·2	1·8	1·9	2·1
	SD	1·8	1·3	1·9	2·4	3·5
	95% conf. interval	−5·1 to +1·9	−2·3 to +2·7	−1·9 to +5·5	−2·8 to +6·6	−4·8 to +9·0

CONCLUSIONS

The time-temperature histories of ideal product shapes with evaporative and convective cooling at the product surface can be described using T_{eq}, f and j values. The equilibrium temperature depends on the ambient air temperature, the relative humidity and the product surface water activity, and will be experimentally tested in a further stage of the study.

Across the ranges tested, the slope of the semi-log plot of unaccompished temperature change versus time for combined evaporative and convective cooling, lies between 1·1 and 2·9 times that of the convection-only cooling. The values of j_{cEvap} and j_{avEvap} are 0·7–1 times the j value for convective only cooling.

When compared with the numerically generated results, the algebraic curve-fit equations generally give good agreement (95% confidence bound of approximately $\pm 5\%$ with the mean difference close to 0%) for a wide range of a_w values, a performance not achieved by other methods. Ranges of applicability are:

T_a	0–15°C
T_{in}	20–50°C
B_i	0·1–10
a_w	0·6–1·0
H_r	0·5–1·0
Shape	infinite slab, infinite cylinder, sphere.

Given likely data uncertainties, particularly for water activity, the equations are probably sufficiently accurate for wide-ranging use as a chilling time prediction method, but this hypothesis requires experimental verification.

REFERENCES

Abdul Majeed, P.M., Srinivasa Murthy, S. & Krisha Murthy, M.V. (1980). Prediction of aircooling characteristics of moist food products. *Trans. Amer. Soc. Agric. Eng.*, **23**, 778–792.

Campanone, L.A., Giner, S.A. & Mascheroni, R.H. (1995). The use of a simulation software to optimise cooling times and to lower weight losses in fruit refrigeration. *Proc. 19th Int. Congr. Refrig.*, **1**, 121–128.

Chau, K.V., Gaffney, J.J. & Baird, C.D. (1985). Transient heat and mass transfer for oranges in closed containers. *Refrig. Sci. Technol.*, 1985-5, 283–290.

Chuntranuluck, S. (1995). Prediction of chilling times of foods subject to both convective and evaporative cooling at the product surface. PhD thesis, Massey University, Palmerston North, New Zealand.

Chuntranuluck, S., Wells, C.M. & Cleland, A.C. (1998a). Prediction of chilling times of foods in situations where evaporative cooling is significant. Part 2, Experimental testing. *J. Food Engng*, **37**, 127–141.

Chuntranuluck, S., Wells, C.M. & Cleland, A.C. (1998b). Prediction of chilling times of foods in situations where evaporative cooling is significant. Part 3, Applications. *J. Food Engng*, **37**, 143–157.

Cleland, A.C. (1990). *Food Refrigeration Processes: Analysis, Design and Simulation*. Elsevier Science, London.

Daudin, J.D. & Kuitche, A. (1995). Chilling of pork carcasses with time-variable conditions: analysis and modelling . *Proc. 19th Int. Congr. Refrig.*, **1**, 129–136.

Daudin, J.D. & Swain, M.V.L. (1990). Heat and mass transfer in chilling and storage of meat. *J. Food Engng*, **12**, 95–115.

Earle, R.L. & Fleming, A.K. (1967). Cooling and freezing of lamb and muttton carcasses. I. Cooling and freezing rates in legs. *Food Technol.*, **21**, 79

Gaffney, J.J., Baird, C.C. & Chau, K.V. (1985). Methods for calculating heat and mass transfer in fruits and vegetables, individually and in bulk. *ASHRAE Trans.*, **91**, 333–352.

James, S.J., Fulton, G.S., Swain, M.V.L. & Burfoot, D. (1988). Modelling the effect of temperature and relative humidity fluctuations on weight loss in retail displays. *Refrig. Sci. Technol.*, 1988-1, 187–194.

Kuitche, A. & Daudin, J.D. (1995). Analyse expérimentale et modélisation des cinétiques de température et de perte de poids de carcasses de lapin pendant la réfrigeration. *Int. J. Refrig.*, **18**, 258–271.

Kuitche, A., Daudin, J.D. & Letang, G. (1996). Modelling of temperature and weight loss kinetics during meat chilling for time-variable conditions using an analytical-based method—I. The model and its sensitivity to certain parameters. *J. Food Engng*, **28**, 55–84.

Kuitche, A., Letang, G. & Daudin, J.D. (1996). Modelling of temperature and weight loss kinetics during meat chilling for time-variable conditions using an analytical-based method—II. Calculations versus measurements on wet plaster cylinders and cast. *J. Food Engng*, **28**, 85–107.

Lin, Z., Cleland, A.C., Serrallach, G.F. & Cleland, D.J. (1993). Prediction of chilling times for objects of regular multi-dimensional shapes using a general geometric factor. *Refrig. Sci. Technol.*, **3**, 259–267.

Radford, R.D., Herbert, L.S. & Lovett, D.A. (1976). Chilling of meat—a mathematical model for heat and mass transfer. *Refrig. Sci. Technol.*, 1976-1, 222–226.

Srinivasa Murthy, S., Krishna Murthy, M.V. & Ramachandran, A. (1976). Heat transfer during aircooling and storing of moist food products—II. Spherical and cylindrical shapes. *Trans. Am. Soc. Agric. Eng.*, **19**, 577–583.